GABAergic neurons intermingled with orexin and MCH neurons in the lateral hypothalamus discharge maximally during sleep

Oum Kaltoum Hassani[1], **Pablo Henny**[1,*], **Maan Gee Lee**[2], and **Barbara E. Jones**[1]

[1] Department of Neurology and Neurosurgery, Montreal Neurological Institute, McGill University, Montreal, Quebec, Canada H3A 2B4

[2] Department of Pharmacology, School of Medicine, Kyungpook National University, Daegu 700-422, South Korea

Abstract

The lateral hypothalamus (LH), where wake-active Orexin (Orx)-containing neurons are located, has been considered a waking center. Yet, melanin-concentrating hormone (MCH)-containing neurons are codistributed therein with Orx neurons and in contrast to them, are active during sleep, not waking. In the present study employing juxtacellular recording and labeling of neurons with Neurobiotin (Nb) in naturally sleeping-waking head-fixed rats, we identified another population of intermingled sleep-active cells, which do not contain MCH (or Orx) but utilize GABA as a neurotransmitter. The "sleep-max" active neurons represented 53% of Nb-labeled MCH (and Orx) immunonegative (−) cells recorded in the LH. For identification of their neurotransmitter, Nb-labeled varicosities of the Nb-labeled/MCH− neurons were sought within sections adjacent to the Nb-labeled soma and immunostained for the vesicular transporter for GABA (VGAT) or for glutamate (VGluT2). A small proportion of sleep-max Nb+/MCH− neurons (19%) discharged maximally during slow wave sleep (SWS, called "S-max") in positive correlation with delta EEG activity and from VGAT staining of Nb-labeled varicosities appeared to be GABAergic. The vast proportion of sleep-max Nb+/MCH− neurons (81%) discharged maximally during paradoxical sleep (PS, called "P-max") in negative correlation with EMG amplitude and from Nb-labeled varicosities also appeared to be predominantly GABAergic. Given their discharge profiles across the sleep-wake cycle, P-max together with S-max GABAergic neurons could thus serve to inhibit other neurons of the arousal systems, including local Orx neurons in the LH. They could accordingly dampen arousal with muscle tone and promote sleep, including PS with muscle atonia.

Keywords

arousal; paradoxical sleep; rat; REM sleep; slow wave sleep; vesicular GABA transporter

Introduction

Since very early studies, the lateral hypothalamus (LH) has been considered to play a critical role in promoting and maintaining wakefulness (see for review, (Jones, 2005; McGinty & Szymusiak, 2005)). Based upon postmortem analysis of lesions in cases of *encephalitis lethargica*, von Economo proposed in the early 20th century (von Economo, 1930) that the posterior hypothalamus with the rostral midbrain constitute a "waking center" that acts in

Correspondence: Dr. Barbara E. Jones, Montreal Neurological Institute, McGill University, 3801 University Street, Montreal, QC, Canada H3A 2B4; Fax: 514-398-5871; barbara.jones@mcgill.ca.
*Present Address: MRC Anatomical Neuropharmacology Unit, University of Oxford, Oxford OX1 3TH, United Kingdom

opposition to the anterior hypothalamus and preoptic region which constitute a "sleep center". The recent discovery of Orexin (Orx, or hypocretin) in neurons within the lateral and posterior hypothalamus fits within this scheme, since this peptide is essential for the maintenance of waking and its absence along with that of its neurons results in narcolepsy with cataplexy in both humans and animals (Chemelli *et al.*, 1999; Lin *et al.*, 1999; Peyron *et al.*, 2000; Thannickal *et al.*, 2000). However, neurons containing melanin-concentrating hormone (MCH) were found to overlap in their distribution with Orx neurons (Broberger *et al.*, 1998) and appeared from c-Fos activation to play an opposite role to the Orx neurons in the regulation of sleep-wake states (Verret *et al.*, 2003; Modirrousta *et al.*, 2005). Using juxtacellular labeling with Neurobiotin (Nb) of recorded neurons in naturally sleeping-waking, head-fixed rats, we recently established that whereas Orx neurons discharge maximally during wake (W) (Lee *et al.*, 2005b), codistributed MCH neurons discharge maximally during sleep, occasionally during slow wave sleep (SWS) and maximally during paradoxical sleep (PS or rapid eye movement, REM sleep) (Hassani *et al.*, 2009b). Yet in addition to many other Orx−negative (−) neurons being maximally active during W (as "W-max") or with cortical activation during W and PS ("WP-max"), we also found in this search many MCH− neurons which were maximally active during sleep ("sleep-max"), including some during SWS (as "S-max") and many during PS (as "P-max"). It thus appeared that within this previously considered waking center, MCH+ and even more numerous MCH− neurons were active during sleep and thus possibly important for the promotion of sleep.

We sought in the present study by application of juxtacellular labeling of recorded neurons, to investigate MCH− sleep-max active neurons and determine their neurotransmitter. For this purpose, we searched for Nb-labeled terminals of Nb+/(Orx−)/MCH− neurons and employed immunostaining for the vesicular transporter protein for GABA (VGAT) (Chaudhry *et al.*, 1998) or for the vesicular transporter for glutamate (VGluT2) (Fremeau *et al.*, 2001; Henny & Jones, 2006b; Henny & Jones, 2006a; Hassani *et al.*, 2009a). With this approach, we identified a substantial group of GABAergic sleep-max-active neurons that are intermingled with Orx and MCH neurons in the LH.

Materials and Methods

Animals, Surgery and Recording

All procedures were approved by the McGill University Animal Care Committee and the Canadian Council on Animal Care. Adult Long-Evans rats (200–250 g, Charles River, St. Constant, Canada) were operated under deep anesthesia (ketamine, xylazine and acepromazine: 65/5/1 mg/kg in a cocktail of 2 ml/kg initial dose and 1 mg/kg booster as needed, i.p.). As described previously (Lee *et al.*, 2004), EEG (epi-dural screws over cortex, including olfactory bulb (OB), anterior medial prefrontal cortex (PF) and retrosplenial cortex (RS)), and EMG electrodes (silver wire loops in neck muscles) were implanted together with a metal u-frame for holding the head by screws to a sliding carriage adapter within the stereotaxic frame. Animals were maintained on a 12:12 hour light-dark schedule with lights on from 7 AM to 7 PM. Under control conditions, they were given free access to food and water when not in the recording chamber. Following recovery from surgery (~2 days), they were gradually habituated to remain quiet with their heads fixed in the carriage adapter while lying within a small Plexiglas box, which prevented twisting but not moving their bodies and limbs. Over a period of 6–9 days, the rats were submitted to daily head-fixation sessions, which increased progressively in duration as long as the rat remained calm. At the end of each session, the rat was given a cereal treat as a reward. Rats learned quickly to sleep for longer periods inside the apparatus (30 min, 1h, 2h, and subsequently 3–6 h).

Following adaptation to head fixation, the rats were once again anesthetized (as above) and operated for drilling holes in the skull (AP −2.8 mm from Bregma, L ±1.3 mm) and opening the dura over the lateral hypothalamic area on each side. After one day of recovery, daily recording sessions of <6 hrs (~11 AM to 5 PM) were performed over a maximum of 4 days.

During recording sessions most rats were maintained under normal conditions with free access to food and water. However, some animals were submitted to mild food restriction or oral ingestion of a sucrose solution preceding the recording session while in search for MCH + neurons, which was not found to affect unit discharge (see (Hassani *et al.*, 2009b)).

Unit Recording and Labeling

As described previously (Lee *et al.*, 2005b; Hassani *et al.*, 2009b), single units were recorded using glass micropipettes (~1 μm tip) that were filled with 0.5 M NaCl and ~5% Neurobiotin (Nb, Vector Laboratories, Burlingame, CA) and an intracellular amplifier (Neurodata IR-283A, Cygnus Technology, Inc., Delaware Water Gap, PA). The unit signal was amplified (x2000) and filtered (0.3–3 KHz) using a CyberAmp380 (Axon Instruments, Union City, CA), then acquired at 16 KHz for on-line viewing with Axoscope (v8.1, Axon Instruments). The unit signal and EEG/EMG were simultaneously acquired and digitized at 8 KHz and 250 Hz, respectively, using EEG and sleep-waking scoring software (Harmonie v5.2, Stellate Co., Montreal, Canada). Video recording of behavior was also acquired simultaneously by the same software.

On the last day of recording, the last cell recorded on each side of the brain during a full sleep-wake cycle was labeled with Nb using the juxtacellular technique. It was estimated that ~80% of units submitted to the juxtacellular labeling protocol were successfully labeled with Nb within the LH in our laboratory (for a total of 121 cells labeled in 77 rats).

Data Analysis

Of all Nb-labeled cells in the LH, 104 met criteria for analysis (including 8 recorded in 5 rats for the present study and 96 recorded in 72 rats for previously published studies (Lee *et al.*, 2005b; Hassani *et al.*, 2009b)). These units were recorded for at least 5 min and during at least one episode of active wake (aW), SWS and PS. Together with the synchronized video images of behavior, records of EEG and EMG were scored by 10 sec epochs for sleep-waking state as described previously (Maloney *et al.*, 1997; Lee *et al.*, 2005a; Hassani *et al.*, 2009b). Wake, SWS and PS states were scored when characteristic EEG/EMG activity occupied >75% of the epoch. Wake was scored with the presence of low voltage fast EEG activity along with moderate to high EMG activity. Active wake (aW) was distinguished from quiet wake (qW) when theta EEG activity (4.5–9.5 Hz) and movement occurred during the wake epoch. The transition to SWS (tSWS) was scored with the appearance of irregular slow EEG activity (<10 Hz) of low to moderate amplitude along with periodic spindles (10–14 Hz), and SWS was scored with the predominance of slow, delta EEG activity (1–4.5 Hz) of high amplitude. The transition to PS (tPS) was scored with the appearance of continuous spindle EEG activity (10–14 Hz), and PS was scored with the presence of continuous rhythmic theta EEG activity (4.5–9.5 Hz) in association with minimal EMG. The average total number of seconds recorded during each stage per unit (aW = 35.91 ± 3.12; qW = 35.22 ± 3.31; tSWS = 80.38 ± 6.54; SWS = 133.12 ± 10.16; tPS = 43.23 ± 2.55; PS = 72.64 ± 5.25) corresponded approximately in percentages to previously obtained percentages of these stages during afternoon recording periods of freely moving rats in our laboratory (Maloney *et al.*, 1999). The unit activity was subsequently analyzed per 10 sec epoch in each sleep-waking state and stage for average discharge rate (ADR, spikes per second or Hz) and instantaneous firing frequency (IFF in Hz, by the reciprocal of the first modal peak of the inter-spike interval histogram). Gamma (30–58 Hz) and delta (1–4.5 Hz) amplitude were

measured by spectral analysis per epoch along with EMG amplitude (30–100 Hz) for correlation with unit spike rate. Classification of units according to the state in which their maximal discharge rate occurred ("max-active") was performed by ANOVA followed by post-hoc paired comparisons (Lee *et al.*, 2004). Other properties were characterized for the maximally active state. According to the IFF, each unit was further classified first as "fast" (>14.5 Hz) or "slow" (<14.5 Hz), and second, as tonic or phasic by comparing the ADR to the IFF (or specifically the corresponding interval of the ADR to the interspike interval distribution). All spikes were averaged across the recording for measurement of the spike duration (from first zero crossing on upward deflection to second zero crossing on second upward deflection on return to baseline, set at 10% of peak amplitude from zero). Electrophysiological properties, ADR, IFF and spike duration of all cells were compared between groups using Student's t-test and in relation to EEG and EMG using Pearson's correlation (Systat v12, San Jose, CA).

Immunohistochemistry

After the recording and labeling of units, the rat was anesthetized with an overdose of sodium pentobarbital (Euthanyl, ~100 mg/kg, i.p.) and perfused with a 4% paraformaldehyde solution. After immersion in 30% sucrose for 2–3 days, brains were frozen for storage and subsequent cutting at 25 μm thick sections. For revelation of Neurobiotin, sections were incubated for 2.5 h in Cy2-conjugated streptavidin (1:1000, Jackson ImmunoResearch Laboratories, West Grove, PA).

For the purpose of identifying the Nb-labeled units (Nb+), the relevant section with the Nb+ cell was processed for dual-immunostaining of Orx and MCH. The section was incubated overnight at room temperature in both goat anti-Orx A antiserum (1:500, Santa Cruz Biotechnology, Santa Cruz, CA) and rabbit anti-MCH antiserum (1:2500, Phoenix Pharmaceuticals, Inc, Belmont, CA) and subsequently for 2 hours in Cy5-conjugated donkey anti-goat antiserum (1:800, Jackson) and in Cy3-conjugated donkey anti-rabbit antiserum (1:1000, Jackson). Nb+ cells were located by epi-fluorescence and photographed using a Nikon Eclipse E800 (Nikon Instruments Inc, Melville, NY) equipped with a digital camera (Optronics, Microfire S99808). The labeled cells were mapped onto a computer resident atlas with the aid of Neurolucida (v7, MicroBrightField, Williston, VT).

For the purpose of identifying the Nb+/Orx−/MCH− cells as GABAergic or glutamatergic, evidence for an Nb-labeled axon or varicosities in the section of the Nb-labeled soma was sought. In only 26 sections was such evidence found such as to process sections adjacent to the Nb-labeled soma for examination of Nb-labeled axonal varicosities. Multiple varicosities were found in 17 cases and processed for immunostaining for the vesicular GABA transporter (VGAT) or vesicular glutamate transporter (VGluT2) in different adjacent sections (Henny & Jones, 2006b; Henny & Jones, 2006a; Hassani *et al.*, 2009a). Sections were incubated with primary antibodies against VGAT (rabbit antiserum, 1:500, Catalog # AB5062P, Millipore, Temecula, CA) or VGluT2 (rabbit antiserum, 1:5000, generous gift from R.H. Edwards and R.T. Fremeau Jr, (Fremeau *et al.*, 2001)) in the presence of 0.1% Triton X-100 (TX) and then with Cy2-conjugated streptavidin for Nb together with Cy3-conjugated donkey anti-Rb antiserum (Jackson).

Results

The new results reported in this study concern MCH− sleep-max-active cells with VGAT+ varicosities that were drawn from a data base of 104 cells which were successfully recorded across a full sleep-wake cycle, labeled with Neurobiotin (Nb), immunohistochemically processed for staining of Orx/MCH and located within the LH region. Of these, 96 cells were originally recorded and tabulated for previously published studies of Orx+ and MCH+

cells (Lee *et al.*, 2005b; Hassani *et al.*, 2009b), and 8 were newly recorded for the present study. Of the 104 cells, 53% (n = 55) were sleep-max-active. A small proportion were S-max (9%, n = 9) and the major proportion, P-max (44%, n = 46, including 7% of neurons that were MCH+ as previously published (Hassani *et al.*, 2009b)). The remaining portions were W-max-active (18%, n = 19, including 6% Orx+ neurons as previously published (Lee *et al.*, 2005b)), WP-max-active (17%, n = 18) or state invariant ("wsp-equivalent" or wsp-eq, 12%, n = 12).

Among 91 cells whose Nb-labeled soma was immunonegative (−) for Orx and MCH, Nb-labeled varicosities (Nb+Vars) were sought and found in sections adjacent to the soma of 17 Nb-labeled cells for examining whether they were VGAT+ or VGluT+ for the present study. During recording sessions, many of these cells were preferentially selected as discharging maximally during sleep, SWS and/or PS. The cells with Nb+Vars included 2 S-max cells and 10 P-max cells, along with 5 other W-max, WP-max or wsp-eq cells. Approximately 13 Nb+Vars were located (on average) per cell in adjacent sections within ~250 μm from that of the Nb+ soma and processed for immunostaining of VGAT. For most cells, Nb+Vars were found in multiple adjacent sections to allow for immunostaining of VGluT2 in additional sections. All Nb+Vars were located within the LH or zona incerta and in the immediate vicinity of where Orx and/or MCH cells are located. In cells judged by their terminals to be VGAT+, immunostaining was established in the majority of the Nb+Vars in the sections processed. Among S-max cells, the Nb+Vars of 2/2 cells were judged to be VGAT+ and VGluT2− (Figs. 1A–C, 2 and 3). Among P-max cells, the Nb+Vars of 8/10 cells were judged to be VGAT+ and VGluT2− (Figs. 1D–F, 2 and 4). The Nb+Vars of two P-max MCH− cells were VGAT− and those of one were also VGluT2+ (not shown). As imaged in Fig. 1 and mapped in Fig. 2, the S-max and P-max, Nb+/MCH−/VGAT+ cells were distributed through the LH in the region where Orx+ and MCH+ neurons are located and were previously recorded (Lee *et al.*, 2005b; Hassani *et al.*, 2009b) and where other sleep-max-active MCH− cells (n = 38) were located. Of the other Orx−/MCH− cells, 1/2 W-max, 0/1 WP-max and 0/2 wsp-eq cells were VGAT+ and VGluT2− (not shown).

Of the Nb+/Orx−/MCH− cells (n = 91) in the LH, 53% (n = 48) discharged maximally during sleep as sleep-max-active cells. Of these, a small number (n = 9) and proportion (19%) discharged maximally during SWS as S-max cells and are described here for the first time. For their neurotransmitter identification, Nb-labeled varicosities could be located in adjacent sections for two of these cells and were found for both to be positively immunostained for VGAT (Fig. 1A–C). The Nb+/Orx−/MCH−/VGAT+ cells were intermingled with Orx+ and MCH+ neurons (Fig. 1A) and codistributed with other S-max MCH− cells in the region of MCH+ and Orx+ neurons (Fig. 2). They showed discharge profiles and properties (Fig. 3) which overlapped with those of other S-max cells (n = 7; Fig. 5A and Figs. S1A and S2A). For this reason and given the small number of VGAT+ cells, the properties of all 9 S-max cells are described. As according to their classification as S-max, all Nb+/MCH− units reached discharge rates during SWS that were maximal and significantly higher than those during aW. On average, the S-max Nb+/MCH−-cells discharged at low rates during aW (mean ± SEM, 1.36 ± 0.96 Hz, n = 9), at relatively high rates during SWS (4.85 ± 2.11 Hz) and at moderate rates during PS (3.63 ± 1.82 Hz), as did also the VGAT+ cells (Figs. 3B and 5A). They also commonly fired during all states, including aW and increased their firing gradually from aW to qW and tSWS to reach maximum rates during SWS (Figs. 3B and 5A and Fig. S3). Many of the S-max MCH− units (6/9, including one VGAT+ cell) continued to fire at relatively high rates during the transition to PS (tPS). They commonly decreased firing to a moderate degree with PS and to a greater degree upon arousal to W from PS (Figs. 3B and 5A and Fig. S3). In most units, their discharge rate was significantly positively correlated (r > + 0.31, p ≤ 0.05) with delta EEG activity across stages (6/9, r = 0.50 ± 0.04; n = 6, including 2 VGAT+ cells), as evident

in the relationship of their average discharge rate to average delta activity across stages (Fig. 5A). Most of the cells were fast spiking neurons (8/9, including the VGAT+ cells). Their instantaneous firing frequency was variable and on average (69.51 ± 22.42 Hz; n = 9) much higher than their average discharge rate, reflecting phasic modulation of their firing (Fig. S2A). Their firing did not show any rhythmicity or relationship to delta EEG activity. The average mean spike duration for all S-max cells was 1.41 ± 0.09 ms (n = 9) and for the VGAT+ cells 1.15 ± 0.11 ms (n =2) (Figs. S1A and S2A).

The largest number (n = 39) and major proportion (81%) of sleep-max MCH− Nb-labeled neurons in the LH discharged maximally during PS as P-max active neurons and are described in detail here for the first time, although mentioned cursorily in a previous report on MCH+ neurons (Hassani *et al.*, 2009b), For the immunohistochemical identification of these cells for the first time in the present report, Nb-labeled varicosities were found in ten of these neurons within adjacent sections. The Nb+Vars of the vast majority of the P-max Nb+/MCH− cells (n = 8) were positively immunostained for VGAT (Fig. 1D–F). The P-max MCH−/VGAT+ neurons were intermingled with Orx+ and MCH+ neurons (Fig. 1D) and codistributed with other P-max MCH− neurons in the region of Orx+ and MCH+ neurons in the LH (Fig. 2). They showed discharge profiles and properties (Fig. 4), which were similar to those of other P-max MCH− neurons (n = 31, Fig. 5B and Figs. S1B and S2B). For this reason, the properties and profiles of all P-max cells are described as a group before those of the specific VGAT+ cells (see paragraph below). As according to their classification as P-max, during PS every unit reached discharge rates that were maximal and significantly higher than those during aW and SWS. On average as a group, the P-max Nb+/MCH− cells (n = 39) discharged at low rates during aW (0.75 ± 0.27 Hz), slightly higher rates during SWS (1.11 ± 0.32 Hz) and relatively high rates during PS (6.46 ± 0.95 Hz) (Fig. 5B). They increased firing gradually during sleep though most markedly during tPS before reaching their maximal firing during PS. Across sleep-wake stages, their discharge rate was significantly (r > 0.31, p ≤ 0.05) negatively correlated with EMG amplitude (in 11/16 units having good quality EMG signal for quantification, r = −0.49 ± 0.04; n = 11), as evident in the average discharge rates in relationship to the average EMG amplitude across sleep-wake stages (Fig. 5B). The majority of them were fast spiking neurons (31/39) and discharged in a phasic mode (33/39) that was reflected by their mean instantaneous firing frequency (54.91 ± 8.36 Hz; n = 39), which was much higher than their average discharge rate during PS (above). Their mean spike duration was 1.49 ± 0.05 ms (n = 39) (Figs. S1B and S2B).

As shown for the representative cell in Fig. 4 (c102u04, also shown in Fig. 1D–F), P-max MCH−/VGAT+ cells discharged minimally during aW and maximally during PS. Even though some cells discharged at a low rate during aW (< 2 Hz, 3/8; Figs. 4B and 5B), most were actually silent during aW (0 Hz, 5/8, with a mean of 0.35 ± 0.23 Hz, n = 8). On the other hand, most discharged during qW at a low rate (< 2 Hz, 6/7, with a mean of 0.26 ± 0.18 Hz; n = 7). They increased their rate progressively during tSWS (0.59 ± 0.29 Hz), SWS (0.77 ± 0.28 Hz) and more markedly during tPS (1.77 ± 0.7 Hz) to reach their highest rates during PS (5.58 ± 1.48 Hz; n = 8; see Figs. 4B and 5B and Fig. S4). Their discharge appeared to be minimal in association with high muscle tone during aW and maximal in association with muscle atonia during PS (Fig. 4A and C). Their discharge rate was significantly (r > 0.31, p < 0.05) negatively correlated with EMG amplitude across sleep-wake stages (in 3 out of 4 cells having good quality EMG recording for quantifying muscle tone, r = −0.50 ± 0.10; n = 3), as evident in the relationship of the average discharge rate and average EMG amplitude across stages (Fig. 5B). They were all fast spiking cells with a mean instantaneous firing frequency (70.29 ± 19.06 Hz; n = 8) that was much higher than their average discharge rate during PS, reflecting their predominantly phasic pattern of discharge. Their firing was neither rhythmic nor related to EEG activity. Their mean spike duration was 1.32 ± 0.06 ms (n = 8, Figs. S1B and S2B). According to their average

discharge rate, instantaneous firing frequency or mean spike duration, they were not significantly different nor could they be distinguished from other P-max MCH− neurons (above, see Fig. S2B).

Discussion

In the present report, we describe for the first time a substantial population of sleep-max-active neurons that are intermingled with Orx+ wake-active neurons and MCH+ sleep-active neurons in the LH and are in the vast majority GABAergic. By their distant or local projections, they could accordingly inhibit neurons of the arousal systems, including Orx neurons, to dampen arousal and promote sleep.

It was at first surprising to find sleep-max-active neurons such as the previously reported MCH+ cells (Hassani *et al.*, 2009b) and the even more numerous MCH− cells in the lateral and posterior hypothalamus, since this region had been considered a 'waking center' acting in opposition to the anterior hypothalamus and preoptic area 'sleep center' (von Economo, 1930; Saper *et al.*, 2001; Alam *et al.*, 2002; Jones, 2005; McGinty & Szymusiak, 2005). On the other hand, substantial numbers of neurons were previously found to express c-Fos during sleep recovery following deprivation, of which less than 10% were MCH+ (Modirrousta *et al.*, 2005). Moreover, sleep-active neurons similar to those described here were previously recorded using similar microelectrodes and estimated to represent a similarly substantial proportion (43% compared to our 53%) of recorded neurons (Koyama *et al.*, 2003), a proportion which interestingly is not different from that of sleep-active neurons recorded in the preoptic region (41%, (Koyama & Hayaishi, 1994)) or basal forebrain (42%, (Hassani *et al.*, 2009a)). Although single unit recording studies can be biased according to the properties of the electrodes and the search criteria of the study, these reports all indicate that significant numbers of sleep-active cells are present in the LH, as they are also in the preoptic and basal forebrain regions. Such intermingling of wake-active and sleep-active neurons in each region indicates that distributed neural networks of reciprocally related elements and not anatomical centers of similarly related elements underlie the regulation of sleep-wake states.

A minor proportion of the Orx−/MCH− cells discharged maximally during SWS, as S-max-active cells (representing 9% of all cells), similarly to previous reports of S-max type cells in the LH (8% of all cells, (Koyama *et al.*, 2003)). Here, we found that all S-max-active MCH− cells for which Nb-labeled terminals could be located, contained VGAT in their terminals suggesting that S-max-active MCH− cells are likely GABAergic. We recently found similar S-max GABAergic cells in the basal forebrain (Hassani *et al.*, 2009a). These S-max cells commonly discharge in positive association with delta EEG activity and could have ascending projections to the cerebral cortex (Manns *et al.*, 2000). They could thus correspond in part to some of the cortically projecting GABAergic cells in the hypothalamus (Vincent *et al.*, 1983). Or, given their local collaterals as visualized here, they could contribute to the inhibition of local W-max, such as Orx neurons, and/or WP-max-active cells in the LH and thus promote SWS. In this process, such S-max GABAergic neurons could contribute to the onset of sleep, the preparation for PS and thus the subsequent completion of the sleep cycle.

The major proportion of the MCH− cells discharged, like the MCH+ cells (Hassani *et al.*, 2009b), maximally during PS, as P-max-active cells (which collectively represent 44% of all cells), similarly to previous reports of P-max type cells in the LH (35% of all cells (Koyama *et al.*, 2003)). Here, we found that 80% of MCH− P-max cells for which Nb-labeled varicosities could be found contained VGAT in their terminals, indicating that the vast majority of MCH− P-max neurons are likely GABAergic. We also recently found P-max

type GABAergic cells in the basal forebrain (Hassani *et al.*, 2009a). In both regions, the discharge of P-max GABAergic neurons is commonly negatively correlated with EMG activity. In the LH, they were mostly silent during aW with high muscle tone, progressively increased their discharge from qW through SWS and tPS to be maximally active during PS with muscle atonia. Their discharge could thus contribute to decreasing activity and muscle tone during sleep culminating in PS.

Such P-max GABAergic LH neurons could give rise to descending projections to the brainstem where they could influence other systems controlling W or PS along with muscle tone. GABAergic hypothalamic neurons have been shown to project caudally into the brainstem to regions of the pons, where neurons involved in promoting W or regulating PS are located (Maloney *et al.*, 1999; 2000; Boissard *et al.*, 2003; Rodrigo-Angulo *et al.*, 2008). W-promoting noradrenergic locus coeruleus neurons which are maximally active during W are tonically inhibited by GABAergic inputs during PS (Nitz & Siegel, 1997; Gervasoni *et al.*, 1998). These inputs could originate in part from PS-active cells in LH which project to the locus coeruleus (Verret *et al.*, 2006; Sapin *et al.*, 2009) and could accordingly correspond to the P-max-active GABAergic cells identified here.

Through local projections or collaterals evidenced here by the Nb-labeled varicosities in the immediate vicinity, the P-max MCH− GABAergic neurons could also inhibit local W-max-active neurons, including the Orx+ neurons (Lee *et al.*, 2005b; Mileykovskiy *et al.*, 2005), with which they are intermingled in the LH. They could accordingly dampen behavioral arousal and muscle tone to promote PS. GABAergic inputs constitute half of the synaptic inputs to most hypothalamic neurons (Decavel & Van den Pol, 1990) and are considerable in number on Orx neurons (Henny & Jones, 2006a). It is likely that many of these GABAergic terminals come from local GABAergic neurons since the most numerous afferents to Orx neurons derive from local hypothalamic neurons (Yoshida *et al.*, 2006). Orx neurons have also been shown to be subject to GABAergic inhibition, mediated through both $GABA_A$ and $GABA_B$ receptors (Eggermann *et al.*, 2003; Xie *et al.*, 2006), that appears to be exerted during sleep (Alam *et al.*, 2005) and could thus come in part from the P-max GABAergic neurons identified here.

The predominant and prominent P-max GABAergic LH neurons discharge in a similar manner to the MCH neurons (Hassani *et al.*, 2009b) and a reciprocal manner to the W-max Orx neurons (Lee *et al.*, 2005b) across sleep-wake stages and in relation to muscle tone and EMG amplitude. Yet, somewhat different from the MCH neurons, the P-max GABAergic cells begin firing during qW and progressively increase firing during SWS such that they appear particularly well suited to inhibit the Orx and other arousal systems and to thereby indirectly modulate muscle tone with behavioral arousal across the sleep-wake cycle. Less numerous S-max GABAergic neurons could also contribute in this process and the initial silencing of the Orx neurons with sleep onset. Collectively, GABAergic sleep-max neurons of the LH could thus participate in dampening the activity of arousal systems, including local Orx neurons, to attenuate behavioral arousal and muscle tone and to promote sleep and PS with muscle atonia.

Supplementary Material

Refer to Web version on PubMed Central for supplementary material.

Acknowledgments

Abbreviations

ADR	average discharge rate
aW	active wake
EEG	electroencephalogram
EMG	electromyogram
IFF	instantaneous firing frequency
LH	lateral hypothalamus
MCH	melanin-concentrating hormone
Nb	Neurobiotin
Nb+Vars	Neurobiotin+ varicosities
OB	olfactory bulb
Orx	orexin
P-max	paradoxical sleep maximally active
PF	prefrontal cortex
PS	paradoxical sleep
qW	quiet wake
REM	rapid eye movement
RS	retrosplenial cortex
S-max	slow wave sleep maximally active
Sleep-max	sleep maximally active
SWS	slow wave sleep
tPS	transition to paradoxical sleep
tSWS	transition to slow wave sleep
VGAT	vesicular GABA transporter
VGluT	vesicular glutamate transporter
W-max	wake maximally active
WP-max	wake and paradoxical sleep maximally active
wsp-eq	wake, slow wave sleep, paradoxical sleep equivalently active

References

Alam MN, Gong H, Alam T, Jaganath R, McGinty D, Szymusiak R. Sleep-waking discharge patterns of neurons recorded in the rat perifornical lateral hypothalamic area. J Physiol. 2002; 538:619–631. [PubMed: 11790824]

Alam MN, Kumar S, Bashir T, Suntsova N, Methippara MM, Szymusiak R, McGinty D. GABA-mediated control of hypocretin- but not melanin-concentrating hormone-immunoreactive neurones during sleep in rats. J Physiol. 2005; 563:569–582. [PubMed: 15613374]

Boissard R, Fort P, Gervasoni D, Barbagli B, Luppi PH. Localization of the GABAergic and non-GABAergic neurons projecting to the sublaterodorsal nucleus and potentially gating paradoxical sleep onset. Eur J Neurosci. 2003; 18:1627–1639. [PubMed: 14511341]

Broberger C, De Lecea L, Sutcliffe JG, Hokfelt T. Hypocretin/orexin- and melanin-concentrating hormone-expressing cells form distinct populations in the rodent lateral hypothalamus: relationship to the neuropeptide Y and agouti gene-related protein systems. J Comp Neurol. 1998; 402:460–474. [PubMed: 9862321]

Chaudhry FA, Reimer RJ, Bellocchio EE, Danbolt NC, Osen KK, Edwards RH, Storm-Mathisen J. The vesicular GABA transporter, VGAT, localizes to synaptic vesicles in sets of glycinergic as well as GABAergic neurons. J Neurosci. 1998; 18:9733–9750. [PubMed: 9822734]

Chemelli RM, Willie JT, Sinton CM, Elmquist JK, Scammell T, Lee C, Richardson JA, Williams SC, Xiong Y, Kisanuki Y, Fitch TE, Nakazato M, Hammer RE, Saper CB, Yanagisawa M. Narcolepsy in orexin knockout mice: molecular genetics of sleep regulation. Cell. 1999; 98:437–451. [PubMed: 10481909]

Decavel C, Van den Pol AN. GABA: a dominant neurotransmitter in the hypothalamus. J Comp Neurol. 1990; 302:1019–1037. [PubMed: 2081813]

Eggermann E, Bayer L, Serafin M, Saint-Mleux B, Bernheim L, Machard D, Jones BE, Muhlethaler M. The wake-promoting hypocretin-orexin neurons are in an intrinsic state of membrane depolarization. J Neurosci. 2003; 23:1557–1562. [PubMed: 12629156]

Fremeau RT Jr, Troyer MD, Pahner I, Nygaard GO, Tran CH, Reimer RJ, Bellocchio EE, Fortin D, Storm-Mathisen J, Edwards RH. The expression of vesicular glutamate transporters defines two classes of excitatory synapse. Neuron. 2001; 31:247–260. [PubMed: 11502256]

Gervasoni D, Darracq L, Fort P, Souliere F, Chouvet G, Luppi PH. Electrophysiological evidence that noradrenergic neurons of the rat locus coeruleus are tonically inhibited by GABA during sleep. Eur J Neurosci. 1998; 10:964–970. [PubMed: 9753163]

Hassani OK, Lee MG, Henny P, Jones BE. Discharge profiles of identified GABAergic in comparison to cholinergic and putative glutamatergic basal forebrain neurons across the sleep-wake cycle. J Neurosci. 2009a; 29:11828–11840. [PubMed: 19776269]

Hassani OK, Lee MG, Jones BE. Melanin-concentrating hormone neurons discharge in a reciprocal manner to orexin neurons across the sleep-wake cycle. Proc Natl Acad Sci U S A. 2009b; 106:2418–2422. [PubMed: 19188611]

Henny P, Jones BE. Innervation of orexin/hypocretin neurons by GABAergic, glutamatergic or cholinergic basal forebrain terminals evidenced by immunostaining for presynaptic vesicular transporter and postsynaptic scaffolding proteins. J Comp Neurol. 2006a; 499:645–661. [PubMed: 17029265]

Henny P, Jones BE. Vesicular glutamate (VGluT), GABA (VGAT), and acetylcholine (VAChT) transporters in basal forebrain axon terminals innervating the lateral hypothalamus. J Comp Neurol. 2006b; 496:453–467. [PubMed: 16572456]

Jones, BE. Basic mechanisms of sleep-wake states. In: Kryger, MH.; Roth, T.; Dement, WC., editors. Principles and Practice of Sleep Medicine. Elsevier Saunders; Philadelphia: 2005. p. 136-153.

Koyama Y, Hayaishi O. Firing of neurons in the preoptic/anterior hypothalamic areas in rat: its possible involvement in slow wave sleep and paradoxical sleep. Neurosci Res. 1994; 19:31–38. [PubMed: 8008233]

Koyama Y, Takahashi K, Kodama T, Kayama Y. State-dependent activity of neurons in the perifornical hypothalamic area during sleep and waking. Neuroscience. 2003; 119:1209–1219. [PubMed: 12831874]

Lee MG, Hassani OK, Alonso A, Jones BE. Cholinergic basal forebrain neurons burst with theta during waking and paradoxical sleep. J Neurosci. 2005a; 25:4365–4369. [PubMed: 15858062]

Lee MG, Hassani OK, Jones BE. Discharge of identified orexin/hypocretin neurons across the sleep-waking cycle. J Neurosci. 2005b; 25:6716–6720. [PubMed: 16014733]

Lee MG, Manns ID, Alonso A, Jones BE. Sleep-wake related discharge properties of basal forebrain neurons recorded with micropipettes in head-fixed rats. J Neurophysiol. 2004; 92:1182–1198. [PubMed: 15028746]

Lin L, Faraco J, Li R, Kadotani H, Rogers W, Lin X, Qiu X, de Jong PJ, Nishino S, Mignot E. The sleep disorder canine narcolepsy is caused by a mutation in the hypocretin (orexin) receptor 2 gene. Cell. 1999; 98:365–376. [PubMed: 10458611]

Maloney KJ, Cape EG, Gotman J, Jones BE. High-frequency gamma electroencephalogram activity in association with sleep-wake states and spontaneous behaviors in the rat. Neuroscience. 1997; 76:541–555. [PubMed: 9015337]

Maloney KJ, Mainville L, Jones BE. Differential c-Fos expression in cholinergic, monoaminergic and GABAergic cell groups of the pontomesencephalic tegmentum after paradoxical sleep deprivation and recovery. J Neurosci. 1999; 19:3057–3072. [PubMed: 10191323]

Maloney KJ, Mainville L, Jones BE. c-Fos expression in GABAergic, serotonergic and other neurons of the pontomedullary reticular formation and raphe after paradoxical sleep deprivation and recovery. J Neurosci. 2000; 20:4669–4679. [PubMed: 10844036]

Manns ID, Alonso A, Jones BE. Discharge profiles of juxtacellularly labeled and immunohistochemically identified GABAergic basal forebrain neurons recorded in association with the electroencephalogram in anesthetized rats. J Neurosci. 2000; 20:9252–9263. [PubMed: 11125003]

McGinty, D.; Szymusiak, R. Sleep-promoting mechanisms in mammals. In: Kryger, MH.; Roth, T.; Dement, W., editors. Principles and Practice of Sleep Medicine. Elsevier Saunders; Philadelphia: 2005. p. 169-184.

Mileykovskiy BY, Kiyashchenko LI, Siegel JM. Behavioral correlates of activity in identified hypocretin/orexin neurons. Neuron. 2005; 46:787–798. [PubMed: 15924864]

Modirrousta M, Mainville L, Jones BE. Orexin and MCH neurons express c-Fos differently after sleep deprivation vs. recovery and bear different adrenergic receptors. Eur J Neurosci. 2005; 21:2807–2816. [PubMed: 15926928]

Nitz D, Siegel JM. GABA release in the locus coeruleus as a function of sleep/wake state. Neuroscience. 1997; 78:795–801. [PubMed: 9153658]

Peyron C, Faraco J, Rogers W, Ripley B, Overeem S, Charnay Y, Nevsimalova S, Aldrich M, Reynolds D, Albin R, Li R, Hungs M, Pedrazzoli M, Padigaru M, Kucherlapati M, Fan J, Maki R, Lammers GJ, Bouras C, Kucherlapati R, Nishino S, Mignot E. A mutation in a case of early onset narcolepsy and a generalized absence of hypocretin peptides in human narcoleptic brains. Nat Med. 2000; 6:991–997. [PubMed: 10973318]

Rodrigo-Angulo ML, Heredero S, Rodriguez-Veiga E, Reinoso-Suarez F. GABAergic and non-GABAergic thalamic, hypothalamic and basal forebrain projections to the ventral oral pontine reticular nucleus: their implication in REM sleep modulation. Brain Res. 2008; 1210:116–125. [PubMed: 18407254]

Saper CB, Chou TC, Scammell TE. The sleep switch: hypothalamic control of sleep and wakefulness. Trends Neurosci. 2001; 24:726–731. [PubMed: 11718878]

Sapin E, Leger L, Berod A, Herman P, Luppi P-H, Peyron C. Localization of hypothalamic GABAergic neurons implicated in Paradoxical (REM) Sleep regulation and their relationship with MCH neurons. Society for Neuroscience Online Abstracts. 2009; 375.22:FF22.

Thannickal TC, Moore RY, Nienhuis R, Ramanathan L, Gulyani S, Aldrich M, Cornford M, Siegel JM. Reduced number of hypocretin neurons in human narcolepsy. Neuron. 2000; 27:469–474. [PubMed: 11055430]

Verret L, Fort P, Gervasoni D, Leger L, Luppi PH. Localization of the neurons active during paradoxical (REM) sleep and projecting to the locus coeruleus noradrenergic neurons in the rat. J Comp Neurol. 2006; 495:573–586. [PubMed: 16498678]

Verret L, Goutagny R, Fort P, Cagnon L, Salvert D, Leger L, Boissard R, Salin P, Peyron C, Luppi PH. A role of melanin-concentrating hormone producing neurons in the central regulation of paradoxical sleep. BMC Neurosci. 2003; 4:19. [PubMed: 12964948]

Vincent SR, Hokfelt T, Skirboll LR, Wu JY. Hypothalamic gamma-aminobutyric acid neurons project to the neocortex. Science. 1983; 220:1309–1311. [PubMed: 6857253]

von Economo C. Sleep as a problem of localization. The Journal of Nervous and Mental Disease. 1930; 71:249–259.

Xie X, Crowder TL, Yamanaka A, Morairty SR, Lewinter RD, Sakurai T, Kilduff TS. GABA(B) receptor-mediated modulation of hypocretin/orexin neurones in mouse hypothalamus. J Physiol. 2006; 574:399–414. [PubMed: 16627567]

Yoshida K, McCormack S, Espana RA, Crocker A, Scammell TE. Afferents to the orexin neurons of the rat brain. J Comp Neurol. 2006; 494:845–861. [PubMed: 16374809]
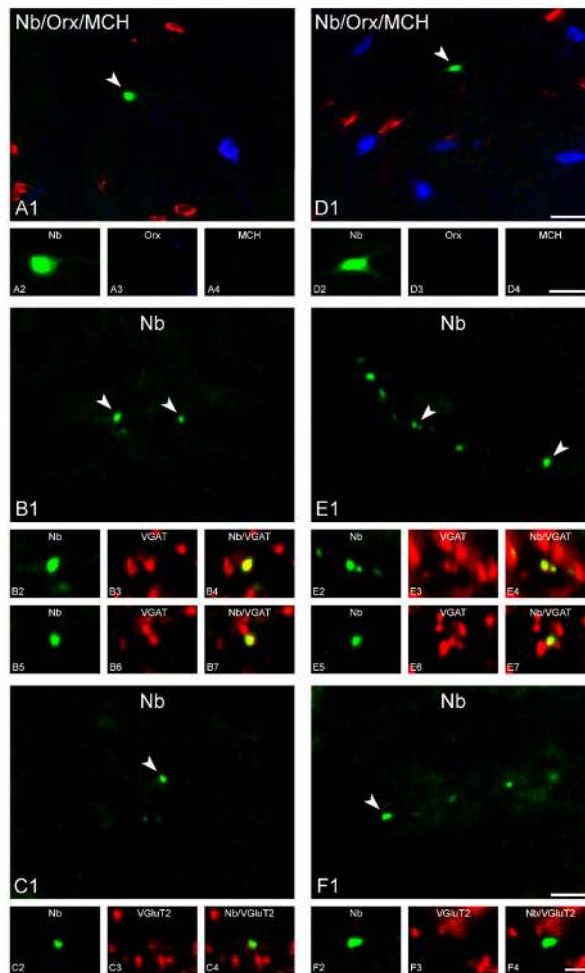
Fig. 1.
Immunostaining of Nb-labeled sleep-active neurons. (A) As shown in merged image (A1), an Nb-labeled cell (#c103u01) that discharged maximally during SWS, as S-max (green, arrowhead) was found intermingled with Orx+ (blue) and MCH+ (red) neurons in the LH. As also shown at higher magnification (A2, A3 and A4), the Nb+ neuron was clearly immunonegative for both Orx and MCH. (B) Found in an adjacent section, the Nb-labeled axon varicosities of the same neuron (B1, green, arrowheads, magnified in B2 and B5) were positively immunostained for VGAT (B3 and B6, red and B4 and B7, yellow in merged images). (C) Another Nb-labeled varicosity of the same neuron (C1, green, arrowhead, magnified in C2), was immunonegative for VGluT2 (C3, red and C4, in merged image). (D) As shown in merged image (D1), an Nb-labeled cell (#c102u04) that discharged maximally during PS, as P-max (green, arrowhead) was intermingled with Orx+ (blue) and MCH+ (red) neurons in the LH. As also shown at higher magnification (D2, D3 and D4), the Nb+ neuron was clearly immunonegative for both Orx and MCH. (E) Found in an adjacent section, the Nb-labeled axon varicosities of the same neuron (E1, green, arrowheads, magnified in E2 and E5) were positively immunostained for VGAT (E3 and E6, red and E4 and E7, yellow in merged images). (F) Another Nb-labeled axon varicosity of the same neuron (F1, green, arrowhead, magnified in F2) was immunonegative for VGluT2 (F3, red and F4, green in merged image). Scale bars in D1, for A1 and D1 = 40 μm; in D4 for insets A2–A4 and D2–D4 = 20 μm; in F1, for B1, C1, E1 and F1 = 5 μm; and in F4 for insets B2–B7, C2–C4, E2–E7 and F2–F4 = 2 μm.
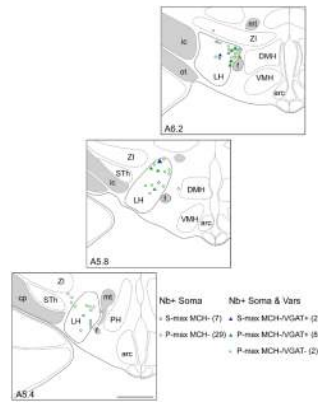
Fig. 2.
Mapping of Nb-labeled (Orx− and) MCH− and VGAT+ sleep-max-active neurons in the LH. Nb-labeled sleep-max neurons were distributed in the region of Orx+ and MCH+ neurons, where Orx+ W-max neurons (Lee *et al.*, 2005b) and MCH+ P-max neurons (Hassani *et al.*, 2009b), were previously recorded. The Nb+/MCH− sleep-max neurons comprised S-max neurons (blue, n = 9) and P-max neurons (green, n = 39). Localization of Nb-labeled varicosities in adjacent sections for some sleep-max neurons allowed identification of (2/2) S-max MCH− neurons as VGAT+ (blue filled triangles, including the cell shown in Fig. 1A–C, depicted here as the largest blue triangle in A5.8). Similarly, localization of Nb-labeled varicosities allowed identification of (8/10) P-max MCH− neurons as VGAT+ (green filled triangles, including the cell shown in Fig. 1D–F, depicted here as the largest green filled triangle in A6.2). The remaining (2/10) P-max MCH− cells were VGAT− (green x's). Cells were mapped according to the appropriate levels (A ~5.4, 5.8, and 6.2 mm from interaural zero) through the LH where Orx+ cells are distributed (Henny & Jones, 2006a). Abbreviations: Arc, arcuate nucleus; cp, cerebral peduncle; DMH, dorsomedial hypothalamic nucleus; f, fornix; ic, internal capsule; LH, lateral hypothalamus; mt, mammillo-thalamic tract; ot, optic tract; PH, posterior hypothalamus; STh, subthalamic nucleus; VMH, ventromedial hypothalamic nucleus; ZI, zona incerta. Scale bar, 1 mm.
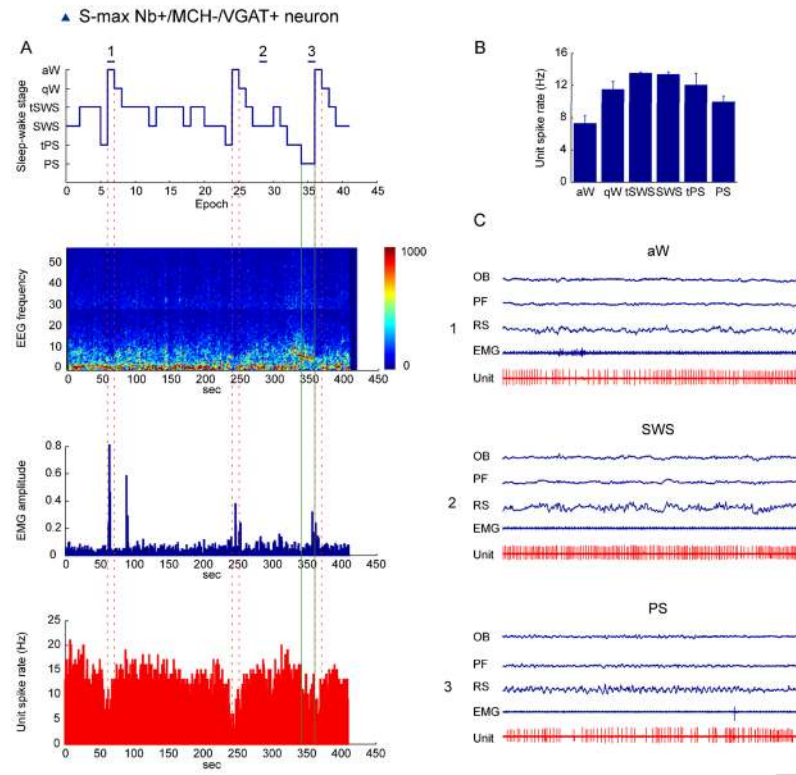
Fig. 3.
Discharge of S-max-active MCH−/VGAT+ cell across sleep-wake states. (A) Data from Nb-labeled unit (c103u01, also shown in Fig. 1A–C) showing the sleep-wake recording scored per 10 sec epochs for sleep and wake stages along with simultaneous EEG frequency and amplitude (μV/Hz with frequency on y axis and amplitude differentially scaled according to color from blue to red, over the low frequency, 0–30 Hz from ~0–100 μV, and the high frequency, 30–60 Hz from ~0–25 μV), EMG amplitude (arbitrary units) and unit spike rate (Hz) over the recording session. Note that the unit discharged at moderately low rates during both aW (showing high EMG activity; periods indicated by red dashed vertical lines) and PS (showing low EMG activity; periods indicated by solid green vertical lines), and at its highest rates during SWS. Across stages, its discharge rate was significantly, positively correlated with delta EEG (r = 0.34). Horizontal lines (marked as 1, 2 and 3) indicate 10 sec recording epochs of aW, SWS and PS respectively shown in *C*. (B) Bar graph showing mean spike rate (Hz) of the unit across sleep-wake stages. Note that the unit fired at a relatively low rate during aW (7.27 Hz), increased its rate through qW, tSWS to reach its maximal rate during SWS (13.35 Hz) and decreased its rate slightly during tPS to reach a lower rate during PS (9.95 Hz). *C,* Polygraphic records from 10 sec epochs (indicated in A) of the unit together with EEG and EMG activity during aW (1), SWS (2) and PS (3). Note that during waking, despite an overall moderate discharge rate, the unit notably slows down its firing during active periods when EMG activity was prominent (C1). It fired continuously and tonically in single spikes during SWS (C2), with an instantaneous firing frequency of 14.9 Hz. It discharged also at moderate rates during PS (C3). Calibrations: horizontal, 1 s; vertical, 1 mV (EEG, EMG), 2 mV (unit). Abbreviations: OB, olfactory bulb; PF, prefrontal cortex; RS, retrosplenial cortex.
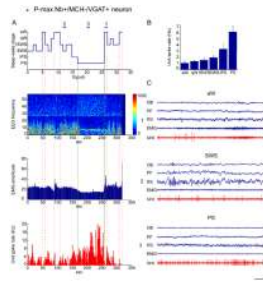
Fig. 4.
Discharge of P-max-active MCH−/VGAT+ cell across sleep-wake states. (A) Data from Nb-labeled unit (c102u04, also shown in Fig. 1D–F) showing the sleep-wake recording scored per 10 sec epochs for sleep and wake stages along with simultaneous EEG frequency and amplitude (μV/Hz with frequency on y axis and amplitude differentially scaled according to color from blue to red, over the low frequency, 0–30 Hz from ~0–100 μV, and the high frequency, 30–60 Hz from ~0–25 μV), EMG amplitude (arbitrary units) and unit spike rate (Hz) over the recording session. Note that the unit showed its lowest firing rates during aW (periods indicated by red dashed vertical lines) and high EMG activity and its highest rates during PS (periods indicated by solid green vertical lines) and low EMG activity. Across stages, its discharge rate was significantly, negatively correlated with EMG amplitude (r = −0.71). Horizontal lines (marked as 1, 2 and 3) indicate 10 sec recording epochs of aW, SWS and PS respectively shown in *C*. (B) Bar graph showing mean spike rate (Hz) of the unit across sleep-wake stages. Note that the unit fired at its lowest rate during aW (1.08 Hz), progressively increased its rate through qW, tSWS and SWS (1.97 Hz) and more markedly increased its rate during tPS to reach its maximal rate during PS (6.22 Hz). (C) Polygraphic records from 10 sec epochs (indicated in A) of the unit together with EEG and EMG activity during aW (1), SWS (2) and PS (3). Note that during waking, the unit fired only minimally and ceased firing altogether during active periods when EMG activity was prominent (C1). It fired periodically in one or two spikes during SWS (C2). It discharged almost continuously and at its highest rates during PS (C3) with an instantaneous firing frequency of 15.38 Hz and tendency toward irregular phasic grouping of spikes. Calibrations: horizontal, 1 s; vertical, 1 mV (EEG, EMG), 2 mV (unit). Abbreviations: OB, olfactory bulb; PF, prefrontal cortex; RS, retrosplenial cortex.
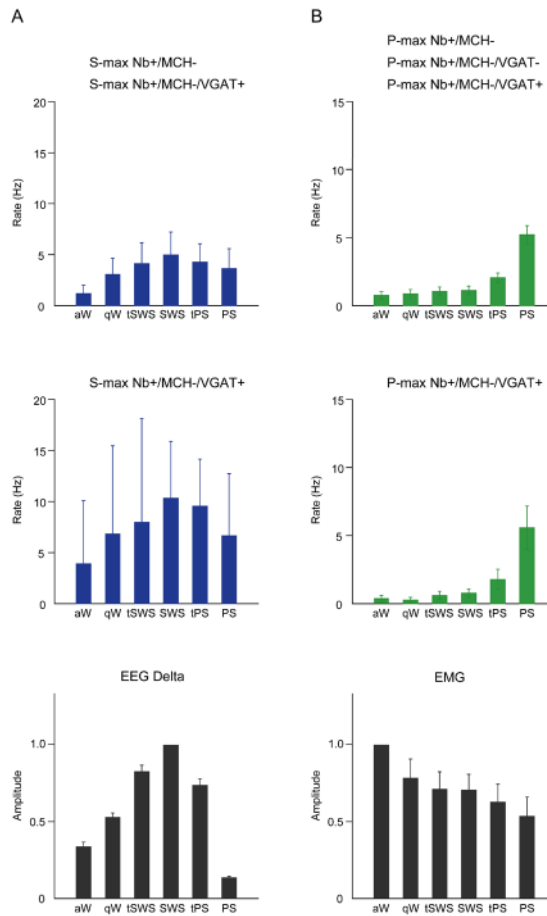
Fig. 5.
Discharge of sleep-max Nb+/MCH− and VGAT+ cells across sleep-wake stages. (A) As a group, all S-max Nb+/MCH− cells, including VGAT+ cells (n = 9) discharged maximally during SWS (top row). S-max VGAT+ neurons (n = 2) discharged with a similar profile (middle row). In all S-max MCH− cells, the discharge rate changed progressively in positive association with delta EEG activity across sleep-wake stages (bottom row, normalized averages from all sleep-max MCH− units). (B) As a group, the P-max Nb+/MCH− cells, including VGAT+ cells (n = 39) discharged maximally during PS (top row). P-max VGAT+ neurons (n = 8) discharged with a similar profile across sleep-wake stages (middle row). In all P-max MCH− cells, the discharge rate changed progressively across sleep-wake stages in negative association with EMG amplitude (bottom row, normalized averages from all sleep-max MCH− units).